# Organic & Biomolecular Chemistry



**PAPER** 

View Article Online



Cite this: Ora. Biomol. Chem., 2022. 20, 6231

# Development of an ATP-independent bioluminescent probe for detection of extracellular hydrogen peroxide†

Justin J. O'Sullivan 🕩 and Marie C. Heffern 🕩 \*

Received 3rd March 2022, Accepted 5th May 2022 DOI: 10.1039/d2ob00436d rsc.li/obc

This work reports a new ATP-independent bioluminescent probe (bor-DTZ) for detecting hydrogen peroxide that is compatible with the Nanoluciferase enzyme. The probe is designed with an arylboronate ester protecting group appended to a diphenylterazine core via a self-immolative phenolate linker. Reaction with hydrogen peroxide reveals diphenylterazine, which can then react with Nanoluciferase to produce a detectable bioluminescent signal. Bor-DTZ shows a dose-dependent response to hydrogen peroxide and selectivity over other biologically relevant reactive oxygen species and can be applied to detect either intra- or extracellular species. We further demonstrate the ability of this platform to monitor fluxes in extracellular hydrogen peroxide in a breast cancer cell line in response to the anticancer treatment, cisplatin.

## Introduction

Hydrogen peroxide (H<sub>2</sub>O<sub>2</sub>) is a key molecule in biological redox metabolism and stress. On the one hand, H2O2 is a hallmark of oxidative stress<sup>2</sup> whereby its generation alongside other reactive oxygen species results in direct or indirect oxidation of various biomolecules such as lipids,3 DNA,4 RNA,5 and proteins. On the other hand, endogenous levels of H<sub>2</sub>O<sub>2</sub> have been shown to play important roles in cellular signaling in processes ranging from immune response to proliferation.<sup>7-11</sup> For example, neutrophils have been shown to utilize NADPH oxidase systems to generate millimolar quantities of H<sub>2</sub>O<sub>2</sub> as a defense against foreign microbes. 12 H<sub>2</sub>O<sub>2</sub> imbalances have been implicated in variety of disease pathologies such as cancer, 13,14 diabetes, 15,16 inflammation 17,18 and cardiovascular diseases. 19,20 Tools for monitoring H<sub>2</sub>O<sub>2</sub> fluxes are vital for understanding the molecular mechanisms at play regarding both the physiological and pathological roles H<sub>2</sub>O<sub>2</sub> plays in biological systems.

Small molecules<sup>21–25</sup> employing various reaction triggers such as sulfonic esters,<sup>22</sup> diketones,<sup>26,27</sup> and arylboronates<sup>28</sup> have been widely employed for fluorescence-based sensing of H<sub>2</sub>O<sub>2</sub>. In particular, the arylboronate reaction-based triggers have been extensively adopted mainly owing to their high selectivity and sensitivity in addition to their fast reaction kine-

Department of Chemistry, University of California Davis, One Shields Drive, Davis, CA 95616, USA. E-mail: mcheffern@ucdavis.edu

† Electronic supplementary information (ESI) available. See DOI: https://doi.org/ 10.1039/d2ob00436d

tics relative to other H<sub>2</sub>O<sub>2</sub>-reactive moieties. <sup>29-32</sup> Although fluorescence-based imaging probes have provided valuable insight into H<sub>2</sub>O<sub>2</sub> dynamics, they are primarily applied to monitoring intracellular H2O2, given that the larger volume and diffuse nature of the extracellular space and extracellular fluids can lead to signal dilution. Aside from fluorescence-based imaging probes researchers have also turned to the development of alternative modalities with improved sensitivity, such as electrochemical sensors, but many of these are not amenable to in vivo work. 33-35

To fill this gap, bioluminescence has become an increasingly favorable candidate for molecular imaging platforms.<sup>36</sup> Bioluminescence results in the emission of photons via the enzymatic oxidation of a small molecule luciferin by its cognate luciferase enzyme. Imaging with this technique offers the benefits of high signal-to-noise ratio as well as the ability to endow cell and tissue specificity through the genetic encoding of the luciferase.37 The phenomenon has been adapted for sensing molecular analytes of interest by chemical modification of the luciferin, termed "caging", which precludes interaction with its luciferase pair. 38,39 Upon chemo-selective reaction with the analyte, the native luciferin is restored and subsequent oxidation by its luciferase results in the production of detectable photons. This strategy has been successfully employed for the detection of intracellular H<sub>2</sub>O<sub>2</sub> using a firefly luciferin caged with an arylboronic acid. 40,41 While capable of detecting intracellular H2O2 and in the tissues of living mice, an inherent property of the firefly luciferin/luciferase system is its dependence on ATP, therefore limiting the probe's applicability to intracellular applications and regimes where ATP

levels are not significantly perturbed. Development of probes for the extracellular space are of particular interest due to the transient nature of signaling biomolecules like H2O2. The ability to monitor extracellular H2O2 would provide valuable insight into both the physiological roles that this oxidative metabolite plays in extracellular signaling as well as a means to monitor oxidative stress in disease progression. Unlike the firefly luciferases, marine luciferases and their derivatives do not require ATP, making these platforms adaptable to extracellular applications. 42,43

To this end, we report the design, synthesis, and evaluation of a new bioluminescence-based probe for detecting H<sub>2</sub>O<sub>2</sub> in the extracellular space using a marine luciferin/luciferase pair. We report a boronate ester caged diphenylterazine (bor-DTZ), a small molecule luciferin with an H2O2-reactive boronate ester and self-immolative linker attached to the carbonyl of the parent diphenylterazine (DTZ). Upon H<sub>2</sub>O<sub>2</sub>-induced oxidative hydrolysis and subsequent self-immolation, DTZ is generated which can then interact with the engineered marine luciferase, Nanoluciferase (Nluc),44 to produce a detectable bioluminescence signal (Scheme 1). We demonstrate the ability of bor-DTZ to selectively detect H<sub>2</sub>O<sub>2</sub> over other biologically relevant ROS and show that it can detect exogenous and endogenous H<sub>2</sub>O<sub>2</sub> in live cells. We further show the probe's utility in

monitoring changes to extracellular H2O2 in response to a clinically relevant cancer treatment in a human breast cancer cell model.

## Results and discussion

#### Synthesis and reactivity of bor-DTZ

The recently engineered Nluc is a marine-based luciferase derived from a deep sea shrimp which has gained attention due to its small size, high thermal stability, and intense luminescence in the presence of its engineered substrate, furimazine, relative to firefly luciferase/luciferin system.44 We recently demonstrated that modifying imidazopyrazinone substrates at the imidazoyl carbonyl with a reactive group responsive to copper(II) could yield caged luciferins compatible with Nluc, with the synthetic imidazopyrazinone, diphenylterazine (DTZ), yielding optimal response among a series of caged imidazopyrazinone derivatives. 45 Thus, to design a bioluminescence agent for the Nluc system that could respond to hydrogen peroxide, we paired the well-studied arylboronate ester cage to diphenylterazine (DTZ) with a self-immolating phenolate linker (Scheme 2). The arylboronate ester cage is expected to undergo selective oxidative hydroxylation by H<sub>2</sub>O<sub>2</sub>,

Scheme 1 Design of bor-DTZ for H<sub>2</sub>O<sub>2</sub>-responsive bioluminescence. Red: H<sub>2</sub>O<sub>2</sub>-responsive cage, blue: self-immolative linker, black: diphenylterazine (DTZ) core.

Scheme 2 Synthesis of bor-DTZ. Reagents and conditions: (i) NBS, CHCl<sub>3</sub>, 3 h; (ii) phenylboronic acid, Pd(PPh<sub>3</sub>)<sub>4</sub>, K<sub>2</sub>CO<sub>3</sub>, 1,4-dioxane, H<sub>2</sub>O, 80 °C, 12 h; (iii) 1,1-diethoxy-3-phenylpropan-2-one, EtOH, H<sub>2</sub>O, cat. HCl, 80 °C, 12 h; (iv) 4-bromomethylphenylboronic acid pinacol ester, Cs<sub>2</sub>CO<sub>3</sub>, KI, MeCN, 12 h.

which in turn triggers an electron cascade to reveal the parent DTZ for recognition by Nluc. We synthesized the native DTZ according to previously published methods 45,46 and then performed a nucleophilic substitution with 4-bromomethylphenylboronic acid pinacol ester under basic conditions to afford bor-DTZ in 18% yield. We attributed the low yield due to a side product where the pinacol ester adds to the alkene at the C2 position as well as DTZ being inherently prone to oxidation. However, it is important to note that for subsequent biological assays, bor-DTZ can be used in concentrations as low as 1 µM such that low milligram quantities of bor-DTZ can be used for hundreds of assays depending on sample size.

To evaluate the reactivity of bor-DTZ, its luminescence output was measured upon addition of analytes of interest in the presence of purified recombinant Nluc (rNluc) in aqueous buffer. Selectivity was assessed by comparing reactivity with H<sub>2</sub>O<sub>2</sub> to a panel of reactive oxygen species as well as glutathione, a biologically relevant reducing agent. The normalized total photon flux was determined by calculating the area under the curve of the kinetic reading over 30 minutes and normalizing values from all ROS tested to that of bor-DTZ alone (Fig. 1a). A representative kinetic curve for bor-DTZ in the presence of 100  $\mu$ M H<sub>2</sub>O<sub>2</sub> can be seen in the ESI (Fig. S1†). We observed that bor-DTZ exhibits exceptional selectivity towards H2O2 relative to the other ROS tested. We confirmed that the turn-on response was due to H2O2 by observing a loss in signal upon addition of catalase, an enzyme that rapidly degrades H2O2. The DTZ/Nluc system has been previously reported to have a  $\lambda_{max}$  of 500 nm. <sup>46</sup> The **bor-DTZ**/Nluc system similarly yielded a  $\lambda_{max}$  emission of 500 nm in the presence of H<sub>2</sub>O<sub>2</sub> (Table S1†), further confirming that the parent DTZ is released upon reaction with the analyte. Moreover, bor-DTZ demonstrated a dose-dependent response to H2O2 from 50-250 μM (Fig. 1b), which is within a biologically-relevant range areas of interest such tumor microenvironment. 47-49 A 10-fold change in molar luminescence is observed from the lower limit of detection (10 µM  $H_2O_2$ ) to the point of signal saturation (250  $\mu$ M) (Table S1†).

We next assessed whether the signal produced by bor-DTZ was affected by ATP. Previously reported bioluminescence probes for H<sub>2</sub>O<sub>2</sub> rely on the firefly luciferase enzyme, which utilizes ATP as a cofactor. The need for ATP limits the probe to mainly intracellular applications where ATP is abundant; additionally, various cellular processes can result in significant changes to ATP levels, making this cofactor a confounding variable for firefly luciferase-based sensors. Both in absence and presence of H<sub>2</sub>O<sub>2</sub>, bor-DTZ shows no significant alterations in signal when ATP is added (Fig. 1c), confirming the expected ATP-independent behavior of the probe.

#### Detection of intracellular H2O2 by bor-DTZ

Having established the selectivity and sensitivity of bor-DTZ towards H<sub>2</sub>O<sub>2</sub> in buffer we next evaluated the H<sub>2</sub>O<sub>2</sub> responsiveness in cells. We utilized a breast cancer cell line, MDA-MB-231, engineered to express Nluc intracellularly (Nluc MDA-MB-231). To stimulate an increase in intracellular H<sub>2</sub>O<sub>2</sub> we treated cells with 500 μM paraquat for 24 hours, which generates intracellular ROS through disruption of mitochondrial respiration.50 We monitored light output in the presence of bor-DTZ, and analogous experiments were performed using the parent DTZ. The data is presented as the ratio of the area under the curve of the 1 hour luminescence of bor-DTZ: DTZ in order to normalize for any changes in Nluc expression or cell proliferation due to paraquat treatment (Fig. 2a). Representative kinetic curves for the luminescence of both bor-DTZ and DTZ are presented in the ESI (Fig. S2†). Indeed, **bor-DTZ** detected a significant (p < 0.005) increase in the signal of paraquat-treated cells relative to untreated cells showing the biological utility of this probe in cell-based models. As this particular cell line is expressing a form of Nluc without a secretion signaling domain the observed signal indicates that bor-DTZ is able to diffuse through the cell membrane. Additionally, the cells are washed with PBS prior to imaging in order to remove any extracellular hydrogen peroxide or Nluc that may be present. We also performed an experiment to assess the toxicity of bor-DTZ towards the cells

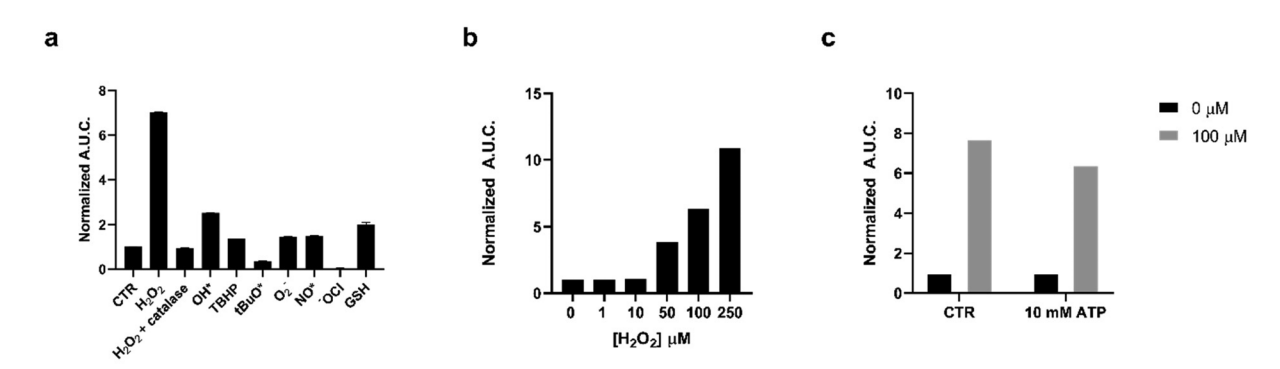
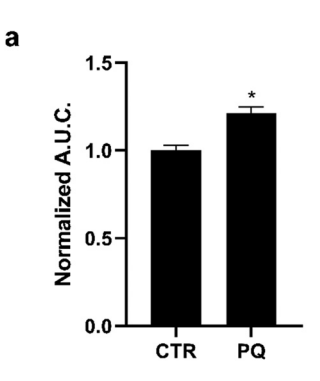


Fig. 1 Reactivity of bor-DTZ (1 µM) reported as calculated area under the curve of luminescence output over 20 minutes in the presence of analytes and rNluc (0.4 µg mL<sup>-1</sup>), normalized to bor-DTZ in the absence of analytes; all solutions were prepared in DPBS, pH 7.4, 37 °C. (a) Reactivity of bor-DTZ in the presence of various biologically relevant ROS (100 µM) and glutathione (GSH, 10 mM). Error bars denote n = 3, SEM. (b) Light output of bor-DTZ in the presence of various concentrations of  $H_2O_2$  (0-250  $\mu$ M) and rNluc (0.4  $\mu$ g mL<sup>-1</sup>). (c) Responsiveness of bor-DTZ to  $H_2O_2$  (100  $\mu$ M) in the presence of ATP (10 mM). Data points are normalized to the control without  $H_2O_2$  added.



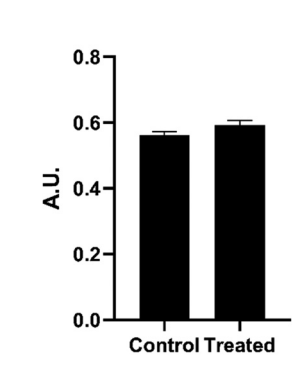


Fig. 2 (a) Calculated ratio of the area under the curve over 1 hour of bor-DTZ: DTZ (10 μM for both) luminescence from MDA-MB-231 cells expressing Nluc in the absence (control, CTR) or presence of 500  $\mu$ M paraquat (PQ) for 24 hours. Error bars denote n=3, SEM. Statistical significance was assessed by calculating p-values using unpaired t-test, \*p < 0.005. Measurements performed in DPBS, pH 7.4, 37 °C. (b) Average absorbance at 490 nm of Nluc MDA-MB-231 cells after an 8-hour incubation with bor-DTZ (10 µM) followed by the addition of MTS for one hour. Error bars denote n = 6

b

using an MTS assay, and found that when Nluc MDA-MB-231 cells are incubated with bor-DTZ (10 µM) for 8 hours there is no significant effect on cell viability (Fig. 2b), suggesting minimal to no toxicity.

#### Detection of extracellular H2O2 by bor-DTZ

To determine the ability of bor-DTZ to detect changes in extracellular H<sub>2</sub>O<sub>2</sub>, we applied bor-DTZ in the media of MDA-MB-231 cells engineered to stably express and secrete Nanoluciferase (secNluc MDA-MB-231). Cells were plated and cultured in Opti-MEM media for 24 hours, then media was removed and placed in a new well plate, H<sub>2</sub>O<sub>2</sub> was spiked in and the samples were treated with bor-DTZ, then analyzed for light output over a 20-minute period. As the cells secrete Nluc, no addition of rNluc was required for these experiments. Furthermore, media was removed from cells and the assay was done in the absence of cells to prevent any signal occurring from intracellular activation. We observed slight increases in light output in the 0-10 μM range followed by large increases from 50-250 μM (Fig. 3a). This range is in line with physiologically-relevant levels of the analyte in tumor microenvironments wherein H2O2 concentrations can reach as high as 50-100 µM. 47-49

To determine if bor-DTZ could detect endogenous levels of H<sub>2</sub>O<sub>2</sub> in the media, the bioluminescent response of the media was measured in the absence or presence of catalase without addition of exogenous H2O2 (Fig. 2b). We observe a drastic decrease in light output in cell media that had been spiked with catalase suggesting bor-DTZ could detect basal levels of H<sub>2</sub>O<sub>2</sub> in the media. Notably, catalase has little to no effect on the native DTZ/Nluc system (Fig. S3†).

As oxidative stress and ROS production is a hallmark of breast cancer,<sup>51</sup> we applied **bor-DTZ** to assess how extracellular H<sub>2</sub>O<sub>2</sub> levels are perturbed in the presence of cisplatin, a wellstudied anti-cancer agent.<sup>52</sup> The secNluc MDA-MB-231 cells

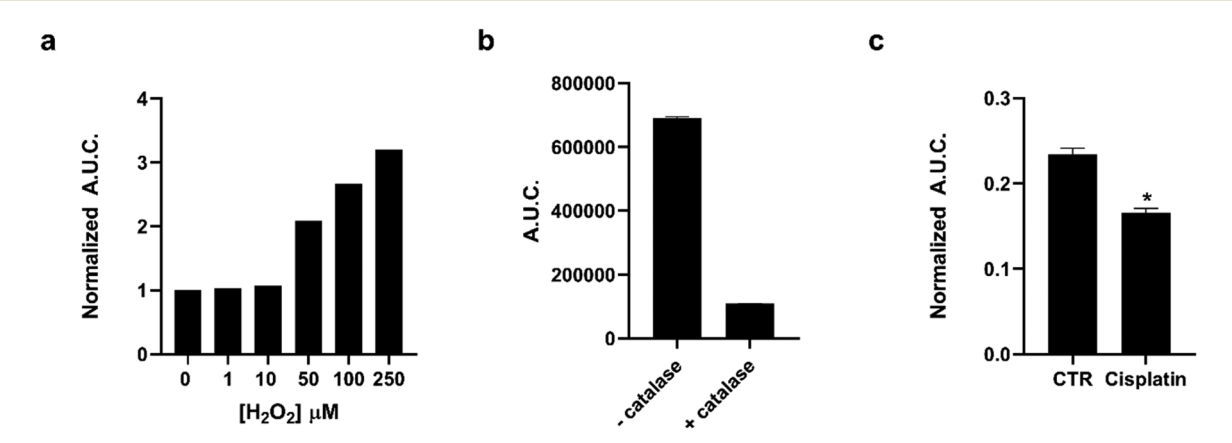


Fig. 3 (a) Dose-dependent light output as monitored by calculated area-under-the-curve for luminescence over 20 minutes of bor-DTZ (1 µM) in the presence of various concentrations of  $H_2O_2$  (0-250  $\mu$ M) in cell media removed from secNluc MDA-MB-231 cells. Data points are normalized to the control without  $H_2O_2$  added. (b) Calculated area under the curve of luminescence over 20 minutes of cell media from secNluc MDA-MB-231 cells in the presence or absence of catalase ( $1 \times 10^4$  U L<sup>-1</sup>) with 1  $\mu$ M bor-DTZ. Error bars denotes SEM, n = 3. (c) Calculated ratio of the area under the curve over 20 minutes of bor-DTZ: DTZ luminescence from secNluc MDA-MB-231 cells treated with cisplatin (30 µM). Error bars denote SEM, n = 3. Statistical significance was assessed by calculating p-values using unpaired t-test, \*p < 0.05. Measurements performed in Opti-MEM, pH 7.4, 37 °C

were plated and treated with cisplatin for 16 hours before removing the media from the cells and monitoring luminescence in the presence of bor-DTZ or the parent DTZ for 20 minutes. The ratio of the area under the curve for bor-DTZ: DTZ was calculated in order to account for any effects that the treatments had on secNluc expression or cell proliferation (Fig. 3c). We observe that cisplatin treatment induces a decrease in light output relative to the control. Interestingly, our previous report on a copper(II)-responsive DTZ showed that cisplatin also decreases extracellular levels of copper(II). 45 These findings provide a basis and tool for further investigations into the interplay between trafficking of H2O2 and copper in both physiological and pathological states. The above study also demonstrates the high-throughput and accessible nature that the bor-DTZ probe offers through use of a 96-well plate format with readings with a luminometer or plate reader. This lays the foundation for a unique new tool for future high-throughput studies investigating the effect of external stimuli on H<sub>2</sub>O<sub>2</sub> dynamics.

# **Experimental methods**

#### General methods

Reactions using moisture- or air-sensitive reagents were carried out in dried glassware under an inert N2 atmosphere. DTZ (4) synthesized according to previously published methods.45,46 Dry solvents were all purchased from Sigma-Aldrich and used immediately. All commercially purchased chemicals were used as received without further purification. 2-aminopyrazine was purchased from Oakwood Products. All other chemicals were purchased from Sigma-Aldrich unless otherwise noted. Silica Gel 60 F254 (precoated sheets, 200 µm thickness, MilliporeSigma) were used for analytical thin layer chromatography. Silica gel sorbent (230-400 mesh, grade 60, ThermoFisher) or aluminum oxide (neutral, Brockmann I, 50-200 µm, grade 60, Sigma-Aldrich) were used for column chromatography. 1H and 13C NMR spectra were collected at room temperature in DMSO-d<sub>6</sub> (Sigma-Aldrich) on a 600 MHz Varian NMR spectrometer. All chemical shifts are reported as  $\delta$ parts per million relative to the residual solvent peak at 2.50 (DMSO-d<sub>6</sub>) for <sup>1</sup>H and 39.52 (DMSO-d<sub>6</sub>) for <sup>13</sup>C. Multiplicities are reported as s (singlet), d (doublet), t (triplet), q (quartet), p (pentet), h (hextet), m (multiplet), dt (doublet of triplets), or br (broad). Heated electrospray ionization mass spectral analyses were performed using an ThermoQ Exactive HF (High field Orbitrap) at the UC Davis Campus Mass Spectrometry Facilities.

### Synthesis of bor-DTZ

Diphenylterazine, 4, (14 mg, 0.037 mmol, 1 equiv.), 4-bromomethylphenylboronic acid pinacol ester (11 mg, 0.037 mmol, 1 equiv.),  $Cs_2CO_3$  (5 mg, 0.015 mmol, 0.4 equiv.), and KI (7 mg, 0.041 mmol, 1.1 equiv.) were added to a flame-dried round-bottom flask that was then purged with  $N_2$ . The reagents were then dissolved in anhydrous acetonitrile (1 mL) and the reaction was allowed to stir overnight. The reaction mixture was

subsequently quenched in 10 mL of water and extracted in DCM (3 × 5 mL). The combined DCM extract was then washed with brine, dried over Na2SO4, and concentrated under reduced pressure. The crude product was then purified by reverse-phase HPLC (isochratic, 80/20 MeCN: H2O over 2 hours on a T3 Atlantis column (Waters)) and dried under reduced pressure to obtain bor-DTZ (4 mg, 18% yield) as a yellow-brown solid.  $^{1}$ H NMR (600 MHz, DMSO-d<sub>6</sub>)  $\delta$  8.83–8.85 (d, 2H), 8.44 (s, 1H), 8.09-8.11 (d, 2H), 7.68-7.70 (d, 2H), 7.50-7.60 (m, 5H), 7.46-7.47 (d, 2H), 7.41-7.43 (t, 1H), 7.27 (m, 4H), 7.18 (m, 1H), 5.25 (s, 2H), 4.07 (s, 2H), 1.27 (s, 12H). <sup>13</sup>C NMR (151 MHz, DMSO-d<sub>6</sub>)  $\delta$  146.08, 139.64, 139.59, 137.25, 137.11, 136.84, 136.19, 135.09, 134.15, 131.55, 130.77, 129.75, 129.17, 129.13, 129.03, 128.88, 128.86, 128.82, 128.74, 126.62, 126.48, 110.99, 84.18, 77.02, 32.95, 25.11. High-resolution mass spectrometry (HRMS) (m/z):  $[M + H]^+$  calculated for: C<sub>38</sub>H<sub>37</sub>BN<sub>3</sub>O<sub>3</sub>, 594.2927; found, 594.2915.

#### In vitro luminescence assays

Milli-Q water (18.2 M $\Omega$ ) was used to prepare all aqueous solutions. Reactive oxygen species solutions were prepared to 10 mM in water. Hydrogen peroxide (H2O2), tert-butyl hydroperoxide (TBHP), and hypochlorite (OCl<sup>-</sup>) stock solutions were prepared from 30%, 70%, and 2-3% aqueous solutions, respectively. Hydroxyl radical (\*OH) and tert-butoxy radical (\*OtBu) were generated in situ by reaction with excess  $Fe(\Pi)$ . Nitric oxide (NO\*) was generated using PROLI NONOate (Cayman Chemical). Superoxide (O<sub>2</sub><sup>-</sup>) was delivered from a stock solution of potassium superoxide (KO2) in DMSO. A 100 µM solution of bor-DTZ was prepared by dissolving bor-DTZ in pure ethanol. A  $0.4 \mu g \text{ mL}^{-1}$  solution of rNluc was prepared by adding 1 μL of 0.4 mg mL<sup>-1</sup> stock solution (Promega, Nano-Glo Assay Kit) into 999 µL of DPBS at pH 7.4. 100 µL of rNluc solution was added to the wells of a white, opaque, flatbottom 96-well plate followed by 1 µL of ROS 10 mM stock solution or 1 μL of a 1 M GSH stock solution. Finally, bor-DTZ (1 µL) was added to all the wells using a multi-channel pipette and mixed well. The bioluminescent signal was immediately measured using a Molecular Devices SpectraMax i3x plate reader at 37 °C for 1 hour. For dose-dependence studies 100× stock solutions of H<sub>2</sub>O<sub>2</sub> were prepared in Millipore water from a 30% (w/w) aqueous solution and 1 µL of these stock solutions were added to 100 µL of rNluc solution in wells of a 96-well white plate. Bor-DTZ (1 μL of a 100 μM solution) was added via a multichannel pipette and the luminescence was immediately measured. For ATP studies a 10 mM solution of ATP was prepared in DPBS pH 7.4 by adding 100 μL of a 100 mM stock (ThermoScientific) into 900 μL of DPBS. To this was added 1 μL of 0.4 mg mL<sup>-1</sup> rNluc (Promega) to get a final volume of 0.4 μg mL<sup>-1</sup> rNluc. The control rNluc solution was prepared to 0.4 μg mL<sup>-1</sup> as described previously and 100 μL aliquots of control and ATP containing solutions were plated in 96-well white plate. Bor-DTZ (1 μL of a 100 μM solution) was added to the wells and the luminescence was measured immediately. When reporting area under the curve, these values were calculated using GraphPad Prism software.

#### Cell culture

MDA-MB-231 cells stably expressing secreted or intracellular Nanoluciferase (secNluc MDA-MB-231 or Nluc MDA-MB-231 respectively) were a kind gift from Drs Gary and Kathy Luker (University of Michigan). Cells were maintained in Dulbecco's modified medium (DMEM, 4.5 g L<sup>-1</sup> glucose) supplemented with 10% fetal bovine serum (FBS) (Gibco) 1× penicillin-streptomycin (Corning), 2 mM L-glutamine (Gibco), 1 mM sodium pyruvate (Gibco) at 37 °C and 5% CO<sub>2</sub>.

### Detecting H<sub>2</sub>O<sub>2</sub> intracellularly in Nluc MDA-MB-231 cells

Cells were plated at 10 000 cells per well in a 96-well white, opaque, flat bottom plate. Twenty-four hours later media was replaced with fresh media and paraquat was added from a freshly prepared stock solution to a final concentration of 500 µM. Cells were then incubated for 24 hours and then the media was removed and washed with warm DPBS before adding 100 µL of fresh DPBS to wells. Bor-DTZ (1 µL of a 1 mM solution) was added to wells and luminescence was measured immediately over one hour.

#### MTS assay of Bor-DTZ treated Nluc MDA-MB-231 cells

Cells were plated at 10 000 cells per well in a 96-well black, clear bottom plate. Twenty-four hours later the media was replaced with fresh media (containing no FBS) and Bor-DTZ (stock solution in ethanol) was added to wells at a final concentration of 10 µM and the plate was incubated for 8 hours in a 37 °C incubator and 5% CO<sub>2</sub>. Following incubation MTS (CellTiter 96, Promega) was added to wells according to the manufacturers protocol. The plate was incubated for one hour at 37 °C before measuring the absorbance at 490 nm on a Molecular Devices SpectraMax i3x.

#### Detecting H<sub>2</sub>O<sub>2</sub> in media of secNluc MDA-MB-231 cells

Cells were plated at 10 000 cells per well in a 96-well black clear bottom plate. Twenty-four hours later the media was removed from the wells and added to a fresh 96-well white, opaque, flat bottom plate. Catalase (Sigma Aldrich) was added to wells in triplicate to a final concentration of  $1 \times 104$  U L<sup>-1</sup> from a stock solution. Following this bor-DTZ (1 µL of a 100 µM solution) was added to wells and luminescence was measured immediately. For dose-response experiments 100× solutions of H<sub>2</sub>O<sub>2</sub> were prepared in water and 1 µL of this was added to secNluc MDA-MB-231 cells 24 hours after plating as previously described. Bor-DTZ (1 µL of a 100 µM solution) was added to wells and luminescence was measured immediately.

### Monitoring secNluc MDA-MB-231 response to cisplatin

Cells were plated at 10 000 cells per well in a 96-well, white, opaque flat-bottom plate. Eight hours later, the media was removed, and the cells were washed with pre-warmed (37 °C) DPBS and 100 µL of Opti-MEM (Gibco) was added to each well. A 3 mM solution of *cis*-platin was prepared in water. 1  $\mu$ L of this was added to the wells for a final concentration of 30  $\mu$ M cisplatin. At the 16-hour time point solutions of 100 µM borDTZ and 100 µM DTZ (in ethanol) were prepared and 1 µL was added per well per treatment (n = 3). Luminescence was immediately recorded as previously described. The area under the curve was calculated using GraphPad Prism software and the ratio of the A.U.C. from bor-DTZ to DTZ was calculated.

# Conclusions

We have demonstrated the design, synthesis, and evaluation of a new bioluminescent probe, bor-DTZ, for monitoring H<sub>2</sub>O<sub>2</sub> in vitro in an ATP-independent manner. Bor-DTZ shows a high level of selectivity towards H<sub>2</sub>O<sub>2</sub> over other biologically relevant reactive oxygen species and shows sensitivity down to the lowmid μM range. The probe can detect H<sub>2</sub>O<sub>2</sub> in either intracellular or extracellular environments based on where the Nluc enzyme is expressed. We also demonstrate that bor-DTZ can be applied to a 96 well-plate for cell-based assays for highthroughput analysis of H<sub>2</sub>O<sub>2</sub> dynamics in a cancer cell line.

Bioluminescence-based sensing of H2O2 offers the advantages of in vivo compatibility as well as high sensitivity due to near-zero background and signal output that does not require an excitation light source. Among the caged bioluminescence agents that have been reported, bor-DTZ is one of the first diphenylterazine-based imaging probes to be paired with the bright, thermostable Nluc. The ATP-independent nature of Nluc allows bor-DTZ to be used in both intracellular and extracellular applications broadening the scope of currently available tools for H2O2. Paired with Nluc and emerging analogs for deep-tissue imaging, bor-DTZ has broad potential for investigating oxidative biology in both cell-based and live-animal studies.

## Author contributions

J. J. O. and M. C. H. designed all experiments. J. J. O. performed all experiments and data collection. J. J. O. and M. C. H. analyzed the data. J. J. O. took the lead in writing the manuscript, and J. J. O. and M. C. H. wrote and edited the manuscript. M. C. H. conceived the study and was the major supervisor on overall direction of the study.

# Conflicts of interest

The authors report no conflicts of interest.

# Acknowledgements

This work was supported by the National Institute of Health (NIH MIRA 5R35GM133684-02), the National Science Foundation (NSF CAREER 2048265). We also thank the Hartwell Foundation for their generous support for M. C. H. as a Hartwell Individual Biomedical Investigator, as well as the UC Davis CAMPOS Program and the University of California's

Presidential Postdoctoral Fellowship Program for their support of M. C. H. as a CAMPOS Faculty Fellow and former UC President's Postdoctoral Fellow, respectively. This work was also supported in part by gift funds from the UC Davis Comprehensive Cancer Center. We thank Dr's Gary and Kathy Luker (University of Michigan) for gifting MDA-MB-231 cell lines stably expressing secreted Nanoluciferase. We thank Samuel Janisse for running HRMS.

## Notes and references

- 1 R. P. Brandes, N. Weissmann and K. Schröder, Free Radical Biology and Medicine Nox Family NADPH Oxidases: Molecular Mechanisms of Activation, *Free Radicals Biol. Med.*, 2014, **76**, 208–226.
- 2 M. Rojkind, J. Domínguez-rosales, N. Nieto and P. Greenwel, Role of Hydrogen Peroxide and Oxidative Stress, Cell. Mol. Life Sci., 2002, 59, 1872–1891.
- 3 Y. H. Siddique, G. Ara and M. Afzal, Estimation of Lipid Peroxidation Induced by Hydrogen Peroxide in Cultured Human Lymphocytes, *Dose-Response*, 2012, **10**, 1–10.
- 4 M. Valverde, J. Lozano-salgado, P. Fortini, M. A. Rodriguezsastre, E. Rojas and E. Dogliotti, Hydrogen Peroxide-Induced DNA Damage and Repair through the Differentiation of Human Adipose-Derived Mesenchymal Stem Cells, *Stem Cells Int.*, 2018, 2018, 1615497.
- 5 M. Liu, X. Gong, R. K. Alluri, J. Wu, T. Sablo and Z. Li, Characterization of RNA Damage under Oxidative Stress in Escherichia Coli Min, *Biol. Chem.*, 2012, **393**(3), 123–132.
- 6 H. Zhu, T. Tamura, A. Fujisawa, Y. Nishikawa, R. Cheng, M. Takato and I. Hamachi, Imaging and Profiling of Proteins under Oxidative Conditions in Cells and Tissues by Hydrogen-Peroxide-Responsive Labeling, *J. Clin. Exp. Hepatol.*, 2020, 142, 15711–15721.
- 7 J. R. Stone and S. Yang, Hydrogen Peroxide: A Signaling Messenger, *Antioxid. Redox Signal.*, 2006, **8**(3), 243–270.
- 8 C. Lennicke and H. M. Cocheme, Review Redox Metabolism: ROS as Specific Molecular Regulators of Cell Signaling and Function, *Mol. Cell*, 2021, **81**, 3691–3707.
- 9 B. D. Autréaux and M. B. Toledano, REVIEWS ROS as Signalling Molecules: Mechanisms That Generate Specificity in ROS Homeostasis, *Nat. Rev. Mol. Cell Biol.*, 2007, 8, 813–824.
- 10 T. G. Cotter and D. R. Gough, Hydrogen Peroxide: A Jekyll and Hyde Signalling Molecule, *Cell Death Dis.*, 2011, 2, 1–8.
- 11 F. Antunes and P. M. Brito, Redox Biology Quantitative Biology of Hydrogen Peroxide Signaling, *Redox Biol.*, 2017, 13, 1–7.
- 12 S. G. Rhee, H<sub>2</sub>O<sub>2</sub>, a Necessary Evil for Cell Signaling, *Science*, 2006, 312(5782), 1882–1884.
- 13 A. Gupte and R. J. Mumper, Elevated Copper and Oxidative Stress in Cancer Cells as a Target for Cancer Treatment, *Cancer Treat. Rev.*, 2009, 35(1), 32–46.
- 14 T. Finkel, M. Serrano and M. A. Blasco, The Common Biology of Cancer and Ageing, *Nat. Rev.*, 2007, **448**, 767–774.

- 15 W. Wang, W. Jiang, G. Mao, M. Tan, J. Fei, Y. Li and C. Li, Monitoring the Fluctuation of Hydrogen Peroxide in Diabetes and Its Complications with a Novel Near-Infrared Fluorescent Probe, *Anal. Chem.*, 2021, 93, 3301– 3307
- 16 N. Houstis, E. D. Rosen and E. S. Lander, Reactive Oxygen Species Have a Causal Role in Multiple Forms of Insulin Resistance, *Nature*, 2006, 440, 944–948.
- 17 C. Wittmann, P. Chockley, S. K. Singh, L. Pase, G. J. Lieschke and C. Grabher, Hydrogen Peroxide in Inflammation: Messenger, Guide, and Assassin, Adv. Hematol., 2012, 2012, 1–6.
- 18 M. Mittal, M. R. Siddiqui, K. Tran, S. P. Reddy and A. B. Malik, Reactive Oxygen Species in Inflammation and Tissue Injury, *Antioxid. Redox Signal.*, 2014, 20(7), 1126– 1167.
- 19 B. Steinhorn and T. Michel, Chemogenetic Generation of Hydrogen Peroxide in the Heart Induces Severe Cardiac Dysfunction, *Nat. Commun.*, 2018, 9, 4044.
- 20 D. Horwitz, N. A. Sherman and D. Horwitz, Hydrogen Peroxide Cytotoxicity in Cultured Cardiac Myocytes Is Iron Dependent, Am. J. Physiol.: Heart Circ. Physiol., 1994, 226(1), 121–127.
- 21 E. V. Lampard, A. C. Sedgwick, X. Sun, K. L. Filer and S. C. Hewins, Boronate-Based Fluorescence Probes for the Detection of Hydrogen Peroxide, *ChemistryOpen*, 2018, 262– 265.
- 22 H. Maeda, Y. Fukuyasu, S. Yoshida, M. Fukuda, K. Saeki, H. Matsuno, Y. Yamauchi, K. Yoshida, K. Hirata and K. Miyamoto, Fluorescent Probes for Hydrogen Peroxide Based on a Non-Oxidative Mechanism, *Angew. Chem.*, 2004, 43, 2389–2391.
- 23 B. C. Dickinson, C. Huynh and C. J. Chang, A Palette of Fluorescent Probes with Varying Emission Colors for Imaging Hydrogen Peroxide Signaling in Living Cells, J. Am. Chem. Soc., 2010, 23, 5906–5915.
- 24 M. C. Y. Chang, A. Pralle, E. Y. Isacoff and C. J. Chang, A Selective, Cell-Permeable Optical Probe for Hydrogen Peroxide in Living Cells, *J. Am. Chem. Soc.*, 2004, 2, 15392– 15393.
- 25 N. Soh, Recent Advances in Fluorescent Probes for the Detection of Reactive Oxygen Species, *Anal. Bioanal. Chem.*, 2006, 386, 532–543.
- 26 X. Xie, T. Wu, Y. Li, M. Li, Q. Tan, X. Wang and B. Tang, Rational Design of an α-Ketoamide-Based Near-Infrared Fluorescent Probe Speci Fi c for Hydrogen Peroxide in Living Systems, *Anal. Chem.*, 2016, 88, 8019–8025.
- 27 M. Abo, Y. Urano, K. Hanaoka, T. Terai, T. Komatsu and T. Nagano, Development of a Highly Sensitive Fluorescence Probe for Hydrogen Peroxide, *J. Am. Chem. Soc.*, 2011, **133**, 10629–10637.
- 28 V. Carroll, B. W. Michel, J. Blecha, H. Vanbrocklin, K. Keshari, D. Wilson and C. J. Chang, A Boronate-Caged [18 F]FLT Probe for Hydrogen Peroxide Detection Using Positron Emission Tomography, J. Am. Chem. Soc., 2014, 136(42), 14742–14745.

- 29 E. W. Miller, A. E. Albers, A. Pralle, E. Y. Isacoff and C. J. Chang, Boronate-Based Fluorescent Probes for Imaging Cellular Hydrogen Peroxide, *J. Am. Chem. Soc.*, 2005, 127(47), 16652–16659.
- 30 A. R. Lippert, G. C. Van De Bittner and C. J. Chang, Boronate Oxidation as a Bioorthogonal Reaction Approach for Studying the Chemistry of Hydrogen Peroxide in Living Systems, *Acc. Chem. Res.*, 2011, 44(9), 793–804.
- 31 M. S. Purdey, H. J. Mclennan, M. L. Sutton-mcdowall, D. W. Drumm, X. Zhang, P. K. Capon, S. Heng, J. G. Thompson and A. D. Abell, Sensors and Actuators B: Chemical Biological Hydrogen Peroxide Detection with Aryl Boronate and Benzil BODIPY-Based Fluorescent Probes, Sens. Actuators, B, 2018, 262, 750–757.
- 32 Y. Chen, X. Shi, Z. Lu, X. Wang and Z. Wang, A Fluorescent Probe for Hydrogen Peroxide in Vivo Based on the Modulation of Intramolecular Charge Transfer, *Anal. Chem.*, 2017, **89**, 5278–5284.
- 33 S. Hosogi, Y. Marunaka, E. Ashihara and T. Yamada, Plasma Membrane Anchored Nanosensor for Quantifying Endogenous Production of H<sub>2</sub>O<sub>2</sub> in Living Cells, *Biosens. Bioelectron.*, 2021, 179, 113077.
- 34 T. Zhang, Y. Gu, C. Li, X. Yan, N. Lu, H. Liu, Z. Zhang and H. Zhang, Fabrication of Novel Electrochemical Biosensor Based on Graphene Nanohybrid to Detect H 2 O 2 Released from Living Cells with Ultrahigh Performance, *Appl. Mater. Interfaces*, 2017, 9, 37991–37999.
- 35 R. Shen, P. Liu, Y. Zhang, Z. Yu, X. Chen, L. Zhou, B. Nie, J. Chen and J. Liu, Sensitive Detection of Single-Cell Secreted H 2 O 2 by Integrating a Micro Fl Uidic Droplet Sensor and Au Nanoclusters †, Anal. Chem., 2018, 90, 4478–4484.
- 36 C. M. Rathbun and J. A. Prescher, Bioluminescent Probes for Imaging Biology beyond the Culture Dish, *Biochemistry*, 2017, **56**, 5178–5184.
- 37 L. Mezzanotte, M. van't Root, H. Karatas, E. A. Goun and C. W. G. M. Löwik, In Vivo Molecular Bioluminescence Imaging: New Tools and Applications, *Trends Biotechnol.*, 2017, 35(7), 640–652.
- 38 J. Li, L. Chen, L. Du and M. Li, Cage the Firefly Luciferin! A Strategy for Developing Bioluminescent Probes, *Chem. Soc. Rev.*, 2013, 42(2), 662–676.
- 39 X. Yang, Z. Li, T. Jiang, L. Du and M. Li, A Coelenterazine-Type Bioluminescent Probe for Nitroreductase Imaging, *Org. Biomol. Chem.*, 2018, **16**, 146–151.
- 40 G. C. Van De Bittner, E. A. Dubikovskaya, C. R. Bertozzi and C. J. Chang, In Vivo Imaging of Hydrogen Peroxide Production in a Murine Tumor Model with a Chemoselective Bioluminescent Reporter, *Proc. Natl. Acad.* Sci. U. S. A., 2010, 21316–21321.

- 41 G. C. Van De Bittner, C. R. Bertozzi and C. J. Chang, Strategy for Dual-Analyte Luciferin Imaging: In Vivo Bioluminescence Detection of Hydrogen Peroxide and Caspase Activity in a Murine Model of Acute In Fl Ammation, *J. Am. Chem. Soc.*, 2013, 135, 1783–1795.
- 42 H. Yeh, Y. Xiong, T. Wu, M. Chen, A. Ji, X. Li and H. Ai, ATP-Independent Bioluminescent Reporter Variants To Improve in Vivo Imaging, *ACS Chem. Biol.*, 2019, **14**, 959–965.
- 43 S. V. Markova, M. D. Larionova and E. S. Vysotski, Shining Light on the Secreted Luciferases of Marine Copepods: Current Knowledge and Applications, *Photochem. Photobiol.*, 2019, 95(2), 705–721.
- 44 M. P. Hall, J. Unch, B. F. Binkowski, M. P. Valley, B. L. Butler, M. G. Wood, P. Otto, K. Zimmerman, G. Vidugiris, T. MacHleidt, *et al.* Engineered Luciferase Reporter from a Deep Sea Shrimp Utilizing a Novel Imidazopyrazinone Substrate, *ACS Chem. Biol.*, 2012, 7(11), 1848–1857.
- 45 J. J. O'Sullivan, V. Medici and M. C. Heffern, A Caged Imidazopyrazinone for Selective Bioluminescence Detection of Labile Extracellular Copper(π), *Chem. Sci.*, 2022, **13**, 4352.
- 46 H. Yeh, O. Karmach, A. Ji, D. Carter, M. M. Martins-green and H. Ai, Red-Shifted Luciferase – Luciferin Pairs for Enhanced Bioluminescence Imaging, *Nat. Methods*, 2017, 14(10), 971–978.
- 47 Q. Chen, C. Liang, X. Sun, J. Chen, Z. Yang, H. Zhao, L. Feng and Z. Liu, H<sub>2</sub>O<sub>2</sub>-Responsive Liposomal Nanoprobe for Photoacoustic Inflammation Imaging and Tumor Theranostics via in Vivo Chromogenic Assay, *Proc. Natl. Acad. Sci. U. S. A.*, 2017, 114(21), 5343–5348.
- 48 Q. Chen, L. Feng, J. Liu, W. Zhu, Z. Dong and Y. Wu, Intelligent Albumin -MnO<sub>2</sub> Nanoparticles as PH-/H<sub>2</sub>O<sub>2</sub>-Responsive Dissociable Nanocarriers to Modulate Tumor Hypoxia for Effective Combination Therapy, *Adv. Mater.*, 2016, 28, 7129-7136.
- 49 T. P. Szatrowski and C. F. Nathan, Production of Large Amounts of Hydrogen Peroxide by Human Tumor Cells, *Cancer Res.*, 1991, **51**, 794–798.
- 50 P. R. Castello, D. A. Drechsel and M. Patel, Mitochondria Are a Major Source of Paraquat-Induced Reactive Oxygen Species Production in the Brain \*, *J. Biol. Chem.*, 2007, 282(19), 14186–14193.
- 51 N. S. Brown and R. Bicknell, Hypoxia and Oxidative Stress in Breast Cancer Oxidative Stress: Its Effects on the Growth, Metastatic Potential and Response to Therapy of Breast Cancer, *Breast Cancer Res.*, 2001, 3(5), 323–327.
- 52 R. S. Polishchuk, Activity and Trafficking of Copper-Transporting ATPases in Tumor Development and Defense against Platinum-Based Drugs, *Cells*, 2019, **8**, 1080.